Polymer 53 (2012) 1267–1276

Contents lists available at SciVerse ScienceDirect

Polymer

journal homepage: www.elsevier.com/locate/polymer

Sorption and transport of methanol and ethanol in H^+-nafion

Qiao Zhao, Nicole Carro, Ho Youn Ryu, Jay Benziger*

Department of Chemical and Biological Engineering, Princeton University, Princeton, NJ 08544, USA

ARTICLE INFO

Article history:
Received 17 November 2011
Received in revised form
25 January 2012
Accepted 25 January 2012
Available online 1 February 2012

Keywords:
Nafion
Methanol
Ethanol

ABSTRACT

Methanol and ethanol sorption and transport in 1100 equivalent weight H+Nafion were compared to water sorption and transport. Sorption isotherms for methanol and ethanol were fit to a solvation shell model, with four molecules in the first solvation shell. The larger molar volume of alcohols resulted in greater swelling from sorption. Proton conductivity is five times greater for water saturated Nafion than alcohol saturated Nafion. Alcohol pervaporation and alcohol vapor permeation is slower than water pervaporation and water vapor permeation. The Nafion/vapor interfacial transport coefficients for alcohols and water scale with vapor pressure. The diffusivity of water is 3–4 times greater than the diffusivity of methanol and ethanol. The results indicate that alcohols sorb by solvating the sulfonic acid groups, similar to the interaction of water with Nafion. Larger alcohol molecules diffuse slower in the hydrophilic channels of Nafion than the smaller water molecules.

1. Introduction

Alcohol fuel cells are attractive because they employ a liquid fuel that has a large energy density [1]. Solutions of methanol or ethanol in water are fed to the anode where the alcohols react with water to make protons and oxidized carbon species. The protons are transported across a Polymer Electrolyte Membrane (PEM) where they react with oxygen to make water. Unreacted alcohol crossover occurs through the PEM that reduces fuel utilization and cell potential [2–4]. The most common PEM employed in methanol or ethanol fuel cells has been Nafion. Nafion is chemically robust and hydrated Nafion has high proton conductivity. However, alcohol crossover is large through Nafion membranes. Substantial research efforts have been devoted in the past decade to developing new PEM materials that would limit methanol crossover (see reference [2] for a review).

A number of researchers have examined the transport of methanol or ethanol from aqueous solutions through Nafion [5–12]. Surprisingly, there are very few fundamental studies of neat alcohol sorption and transport properties in Nafion. A comprehensive understanding of alcohol sorption and transport in PEM materials would be valuable to the development of new materials.

Nafion is a perfluorosulfonated random copolymer that microphase separates into hydrophilic domains consisting of sulfonic acids and polar solutes embedded in a hydrophobic matrix of the tetrafluoroethylene backbone and the perfluoroalkyl ether side chains. Water, methanol and other polar solutes are believed to be sorbed into and transported through the hydrophilic domains. Although the alkyl groups on methanol and ethanol may interact with the hydrophobic phase [4], it is expected that the interaction between the polar hydroxyl group of the alcohol and the polar sulfonate of the sulfonic acid will be dominant.

Several methods have been published in the literature for characterizing methanol crossover from aqueous solutions through Nafion membranes: *in situ* measurements of crossover flux by means of the cathode CO_2 content [13–15], or limiting current [16–18] and *ex situ* measurements using a permeation cell [6,7,11,12,19]. The first method determines the CO_2 flux in the cathode effluent which is equal to the methanol that diffuses from the anode to the cathode. The limiting current method involves feeding neat methanol at the cathode, and letting it crossover to the anode where it can react with water to form protons. The resultant proton current from anode to cathode is proportional to the crossover flux of methanol. These *in situ* methods are complicated by transport through the additional layers of the porous electrode pressed against the membrane. There are also problems arising from incomplete methanol oxidation (methanol oxidation products may be formaldehyde, formic acid and carbon monoxide as well as CO_2). Electro-osmotic drag may also transport alcohol molecules from the anode to the cathode. Methanol transport from aqueous solutions has also been examined *ex situ* by placing a bare membrane between two compartments, one filled with a methanol solution of known concentration and the other with pure liquid water or a dry carrying gas. The methanol flux is determined as functions of liquid composition and temperature. This method is

* Corresponding author. Tel.: +1 6092585416; fax: +1 6092580211.
E-mail address: benziger@princeton.edu (J. Benziger).

0032-3861/$ – see front matter © 2012 Elsevier Ltd. All rights reserved.
doi:10.1016/j.polymer.2012.01.050

intended to mimic the actual conditions in a fuel cell. Pulsed gradient spin echo-NMR has also been applied for measuring self-diffusivity of methanol in Nafion membranes [6,8,10].

The presence of water can significantly complicate the analysis of sorption and transport data. To better understand alcohol sorption and diffusion from mixtures of alcohols and water we suggest it is best to start with characterizing sorption and diffusion of water and alcohol as pure species. Our group has demonstrated that transport of pure water through Nafion is complex, involving interfacial transport, diffusion and polymer relaxation dynamics [20,21]. We build upon that work by asking, *do sorption and transport occur by similar mechanisms as observed for water?*

We present in this paper a comprehensive and systematic study of neat alcohol sorption, steady state pervaporation, vapor permeation, volumetric swelling of alcohol sorption, and the resultant proton conductivity from alcohol sorption into equivalent weight 1100 H+Nafion membranes. All measurements were done under well-controlled temperature and alcohol activity. The Nafion membranes were all prepared by a standard procedure including vacuum annealing at 80 °C that erases memory of microstructural phase separation in Nafion. Dynamic sorption, pervaporation and permeation were done using three membrane thicknesses (51, 127 and 254 μm) to elucidate the rate limiting mechanism of the transport process. Data were analyzed with models originally derived for water sorption and transport. Equilibrium constants for sorption, diffusivity and interfacial mass transport coefficients were calculated for methanol and ethanol in Nafion, and the results were compared with those of water. Alcohol diffusion is slower than water diffusion due to the larger molecular size of the alcohols. Somewhat surprisingly we observed that interfacial transport resistances were similar for water and alcohols.

2. Experimental

2.1. Membrane preparation

Extruded Nafion 1100 Equivalent weight (EW) was purchased from ion power and prepared for testing following our standard cleaning procedure: anneal for 2 h at 80 °C in vacuum for 2 h, boil 1 h in 3% H_2O_2 solution, boil 1 h in deionized (DI) water, boil 1 h in 0.5 M sulfuric acid, boil 1 h in DI water twice. This procedure results in reproducible mechanical and transport property measurements for Nafion films prepared by either extrusion or casting. As discussed by Satterfield and Benziger [22] and Majsztrik et al. [23] annealing above 70–80 °C in vacuum or an inert atmosphere (e.g. N_2) will dissociate the hydrophilic domains removing all memory of microstructure. The resulting clean and protonated Nafion was dried under compression between filter papers under ambient conditions for 2 days. Nafion membranes were cut into squares of 9 cm^2 under ambient conditions before putting into the permeation cell for testing.

Extruded Nafion membranes with dry thicknesses 51 μm (N112), 127 μm (N115) and 254 μm (N1110) were prepared as outlined above and tested. A few membrane samples were prepared by casting 1100 EW Nafion solution into membranes. A total of 5 wt% Nafion solution from Ion Power was cast on a glass plate to a Nafion weight loading of 0.25 g m^2 and dried in vacuum. After vacuum annealing at 80 °C for 2 h the cast Nafion membrane was compared to a N115 membrane. Water sorption, methanol sorption and proton conductivity was the same for both extruded and cast membranes.

2.2. Alcohol sorption and proton conductivity

Equilibrium alcohol uptake and proton conductivity were measured as functions of alcohol pressure at different temperatures using an isometric system [24]. In this system a Nafion membrane is placed in a fixed volume container and evacuated to below 1 Pa (<0.01 mbar) at 80 °C for 2 h to remove all the water and alcohol from the membrane. The pressure container was then cooled to the desired temperature under vacuum. The valve to the vacuum line was shut off and aliquots of alcohol are injected into the pressure vessel and allowed to equilibrate with the Nafion. The resulting pressure is equal to the partial pressure of the alcohol. The difference between the quantity of alcohol injected and the alcohol in the gas phase is equal to the amount of alcohol absorbed by the Nafion. Saturation was evident when the injection of a liquid aliquot did not cause any change in the pressure. We improved the accuracy of the mass uptake experiments compared to previous studies by increasing the mass of ionomer in the isometric cell by a factor of ten.

A piece of polymer in the isometric cell is clamped between electrodes to measure the resistance laterally across a distance of 2 cm. A 500 Hz AC voltage was applied across the PEM and a known resistor placed in series. The voltage drop across the PEM and the known resistor were measured. The membrane resistance was obtained by treating the circuit as a simple voltage divider. By measuring the resistance laterally through a large length and small cross-sectional area the interfacial resistance and capacitance are insignificant compared to the overall impedance [25]; we verified previously that the impedance of Nafion 115 measured laterally is independent of frequency above 10 Hz.

2.3. Volume expansion

The linear expansion coefficient of Nafion was measured as a function of temperature and water activity in a dynamic creep apparatus [26]. Samples were clamped in an environmental chamber, dried in nitrogen at 80 °C for 2 h, brought to the desired temperature in dry nitrogen and then the dry nitrogen was replaced with a controlled alcohol partial pressure in nitrogen stream. The change in length was recorded as a function of time; the equilibrium swelling strain was assumed to be achieved when the rate of swelling was less than 0.001/h. The volume expansion, ΔV, was evaluated from the linear swelling strain, ε, assuming isotropic swelling of Nafion, $(\Delta V/V) = (1+\varepsilon)^3$.

2.4. Sorption/desorption kinetics

Methanol absorption and desorption experiments were carried out with membranes suspended in controlled atmospheres at activity 0 (dry air) or activity 1 (saturated methanol vapor). N112, N115 and N1110 membranes ~1 cm × 3.5 cm were hung on a hook into the container from a bottom-weighing balance, Ohaus AR0640, accurate to 10^{-4} g.

Before sorption experiments, membrane samples were dried in a desiccator over drierite at 70 °C for 2 h. The dry membranes were hung on the hook below the balance and then the saturated vapor container was positioned around the membrane as rapidly as possible. The sample weight was recorded by computer every 2 s for a period of 1500 s. After the methanol uptake experiments the membranes were suspended over methanol liquid in a sealed jar overnight and then reweighed; the saturated membrane mass uptakes were within 5% of those achieved during the absorption experiment.

Desorption experiments were performed after allowing the membrane to equilibrate in the saturated vapor chamber for 2 h after the absorption experiment. The humidified chamber was removed and the immediately replaced with the drying container. The sample weight was recorded every 2 s for a period of 1500 s.

Methanol absorption and desorption experiments were carried out at temperatures from 23 to 60 °C. All experiments were repeated at least two times.

2.5. Pervaporation and vapor permeation measurements

Liquid pervaporation was measured through Nafion membranes using a custom-built permeation cell placed in a Fisher Scientific 838F Isotemp© programmable oven. The details about the permeation cell were described elsewhere [20]. Liquid feeds (methanol, ethanol and water) were introduced from a reservoir into the feed side of the permeation cell by a peristaltic pump with a constant flow rate of ~2 mL/min, which was determined to be in large excess to the pervaporation rate. Dry N_2 gas was fed to the permeate side of the pervaporation cell. A Sensirion SHT75 humidity sensor calibrated for pure methanol vapor was placed downstream of the effluent in an insulated box with temperature maintained at 23 °C to monitor the concentration of methanol. The sensor output voltage was correlated with methanol activity employing a Langmuir adsorption model; experimental values are provided in the Supplementary material. The ethanol flux was measured by trapping the ethanol vapor in a series of dry ice-acetone cold traps.

Vapor permeation of methanol was measured using the same permeation cell [20]. The liquid feed was replaced with partially saturated methanol stream. Nitrogen was passed through two heated bubblers to establish a methanol activity of ~0.95. Methanol activities between 0.00 and 0.9 at the feed side were obtained by mixing methanol saturated N_2 with dry N_2. The total flow rate of methanol vapor feed side was ~ 1 L min^{-1}, which ensured that the change in the activity between the gas entering and leaving the feed side flow channel was less than 5%. The methanol activity in the dry side effluent was monitored by the RH sensor calibrated for methanol.

The permeation rate of methanol from both liquid and vapor can be calculated from the methanol activity measured by the methanol sensor, temperature, and N_2 flow rate at the exit of the dry side with Eq. (1).

$$\text{Flux} = \frac{QP_T}{ART_s}\frac{\alpha_m P_v}{P_T - \alpha_m P_v} \quad (1)$$

where Q is the volumetric flow rate of dry N_2; A is the area of the membrane; P_T is the total pressure of the methanol vapor/gas mixture (1 bar); P_v is the vapor pressure of methanol at the cell temperature; α_m is the activity of methanol in the gas stream; T_s is the standard state temperature of the mass flow controller, 25 °C.

The steady state flux of ethanol was calculated from the net mass (W) collected by four dry ice-acetone the cold traps (Eq. (2)); where t is the duration of collection, A is area of the membrane and M_w is the molecular weight of ethanol.

$$\text{Flux} = \frac{W}{M_w \times A \times t} \quad (2)$$

3. Results

3.1. Sorption, swelling and proton conductivity

Methanol, ethanol and water sorption isotherms in 1100 EW H+Nation as functions of solute activity (a_{solute} = (partial pressure of solute)/(vapor pressure of solute)) at temperatures from 22 °C to 60 °C are shown in Fig. 1. Methanol, ethanol and water sorption isotherms at different temperatures scale with solute vapor pressure; the sorption isotherms are almost independent of temperature when plotted as a function of solute activity. At low solute activity, $a_{solute} < 0.4$, the molar uptakes of methanol, ethanol and water were nearly identical. As solute activity approaches one (saturated vapor) the molar uptake of water was greater than methanol which was greater than ethanol. Fig. 2 compares the swelling strain of Nafion as a function of methanol, ethanol and water activity. The swelling volumes show the opposite trend from molar uptake. Ethanol caused the largest swelling volume, followed by methanol with water having the smallest swelling volume.

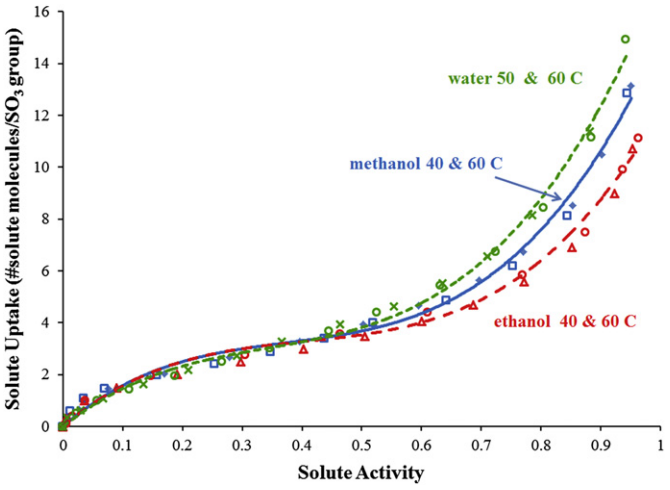

Fig. 1. Methanol, ethanol and water sorption isotherms in 1100 EW H+-Nafion. Sorption isotherms were obtained at: 40 and 60 °C for methanol; 40 and 60 °C for ethanol, and at 50, 60 and 80 °C for water.

The excess volume of mixing of alcohol sorption was determined by taking the difference between the volume of alcohol sorbed and the volume change of the polymer after alcohol sorption [24], and is given by Eq. (3),

$$\Delta V_{mixing} = \frac{\left[(1+\varepsilon)^3 - (1+\varepsilon_0)^3\right] EW}{\lambda \rho_{Nafion}} \quad (3)$$

where ε is the measured linear expansion coefficient, and ε_0 is the linear expansion coefficient assuming ideal mixing, e.g. assuming

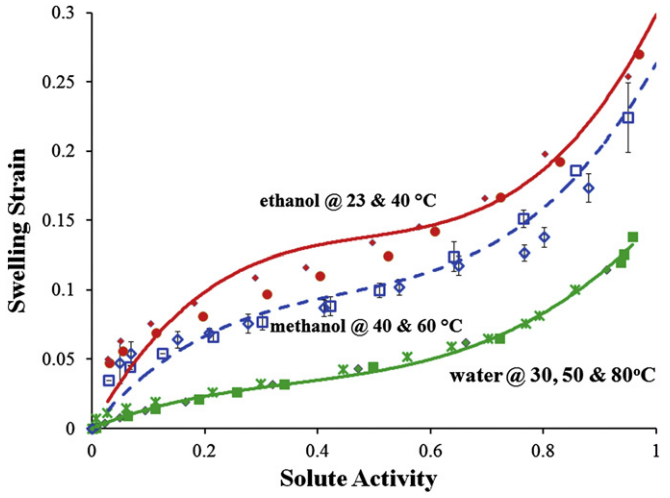

Fig. 2. Linear swelling coefficient for Nafion with sorption of methanol, ethanol and water. Swelling coefficients were obtained at: 23, 40 and 60 °C for methanol; 23 and 40 °C for ethanol, and at 30, 50 and 80 °C for water. The standard error of swelling data is about 7%.

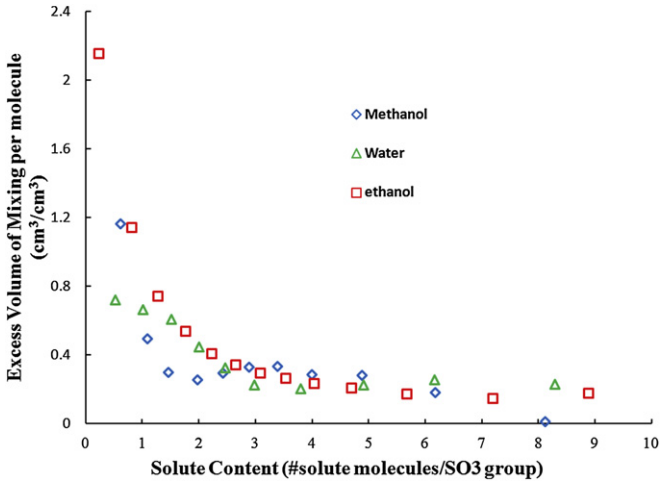

Fig. 3. Excess volume of mixing per unit volume of solute for methanol, ethanol and water sorption in Nafion.

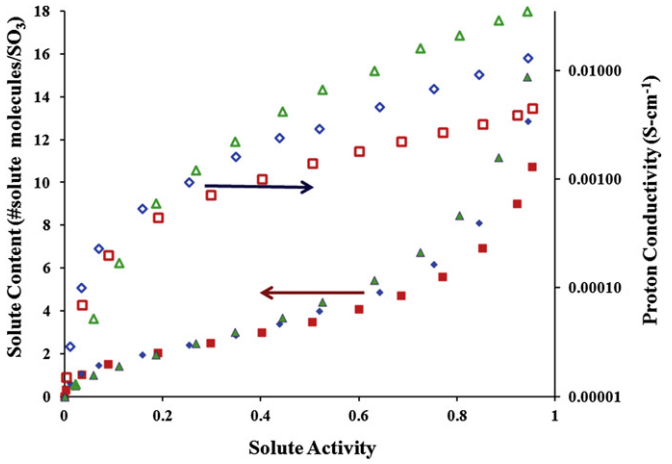

Fig. 4. Proton conductivity of 1100 EW H+-Nafion at 60 °C with methanol, ethanol and water sorbed.

zero excess volume of mixing. The ideal linear expansion coefficient given by Eq. (4) is obtained from the equilibrium mass uptake.

$$(1+\varepsilon_0)^3 = \left(1+\frac{\lambda \rho_{\text{Nafion}} MW_{\text{solute}}}{EW \rho_{\text{solute}}}\right) \tag{4}$$

The excess volumes of mixing, shown in Fig. 3, are greatest for ethanol and least for water. The excess volume of mixing for all three solutes displays similar trend. ΔV_{mixing} is highest when the first solute molecule is absorbed and ΔV_{mixing} decreases rapidly until the concentration of solute content reaches 3–4, beyond which ΔV_{mixing} decreases towards zero with a much smaller slope. Zhao et al. correlated the change in ΔV_{mixing} with the hydration of solute molecules around the sulfonic acid groups [24]. It was concluded that the solute content of 3–4 corresponds to the number of molecules in the first hydration shell. The results reported here indicate that methanol and ethanol exhibits similar packing around the sulfonic acid as water molecules. Coordination of the first alcohol molecule to the SO_3 group requires disruption of the original electrostatic interactions between SO_3 groups and creation of a void. Adding more alcohol molecules lead to more efficient packing, which decreases ΔV_{mixing}. When the first solvation shell is completed, it effectively shields the solute molecules outside from the electrostatic attraction of the acid group, thus those molecules in the second shell and beyond behave close to bulk liquid, and ΔV_{mixing} approaches to zero. This physical picture agrees well with previous simulation results [27,28].

Proton conductivities of Nafion with methanol, ethanol and water sorption, as functions of solute activity at 60 °C are shown in Fig. 4. Proton conductivity increases exponentially with solute activity. For solute activities <0.1 the proton conductivities in Nafion follow the sequence, $\sigma_{\text{Nafion/ethanol}} > \sigma_{\text{Nafion/methanol}} > \sigma_{\text{Nafion/water}}$. At solute activities >0.4 the proton conductivities follow the opposite trend, $\sigma_{\text{Nafion/ethanol}} < \sigma_{\text{Nafion/methanol}} < \sigma_{\text{Nafion/water}}$. Proton conductivity increased with temperature between 22 °C and 60 °C for methanol, ethanol and water. Graphs of the proton conductivities as functions of methanol or ethanol activity and temperature are provided in the Supplementary material; the proton conductivities in saturated vapor are summarized in Table 1.

Protons are conducted through the hydrophilic domains of Nafion electrolytes. The sorption data from Figs. 1 and 2 can be used to determine the volume fractions of the hydrophilic domains (ϕ_+), which is given by the sum of the volume of the sulfonic acid groups and the volume of sorbed water or alcohol divided by the swollen volume of the polymer (Eq. (5)).

$$\phi_+ = \frac{\dfrac{\rho_{\text{polymer}} \bar{V}_{SO_3}}{EW} + \dfrac{\rho_{\text{Nafion}} \bar{V}_{\text{Solute}} \lambda(\pi a_{\text{solute}})}{EW}}{(1+\varepsilon)^3} = \frac{(1+\varepsilon)^3 - 1 + \phi_0}{(1+\varepsilon)^3} \tag{5}$$

The molar volume of the sulfonate group is ~40 cm^3/mol [29]. Fig. 5 plots the conductivity as a function of the hydrophilic volume fraction of the polymer on a linear scale. The data was fit by a percolation model $\sigma(\lambda_{\text{solute}}) = \sigma_0(\phi_+ - \phi_c)^2$, where ϕ_c is the percolation threshold. The lines in Fig. 5 are fits to the conductivity data at 60 °C. The values of intrinsic conductivity, σ_0, and percolation threshold, ϕ_c, for methanol, ethanol and water at different temperatures were evaluated from the conductivity data and have been summarized in Table 1. Within experimental uncertainty the percolation threshold for proton conductivity was 0.1 for all three solutes. The intrinsic conductivities follow the sequence $\sigma_{0,\text{Nafion/ethanol}} < \sigma_{0,\text{Nafion/methanol}} < \sigma_{0,\text{Nafion/water}}$. The intrinsic conductivities for all three solutes increase with increasing temperature. Over the limited range of temperatures studied the percolation thresholds were not dependent on temperature.

3.2. Methanol sorption/desorption kinetics

The normalized mass gain, $(M(t) - M(t \to \infty)) \div (M(t=0) - M(t \to \infty))$, for methanol sorption/desorption at 50 °C for N112 (51 mm thick), N115 (127 mm thick) and N1110 (254 mm thick) membranes as a function of time, is shown in Fig. 6. The normalized mass loss for methanol desorption from N115 at 50 °C is also shown in Fig. 6. Methanol sorption into H+-Nafion is slower than methanol

Table 1
Intrinsic conductivities and percolation threshold volume fractions.

Solute	Temperature (°C)	Proton conductivity at saturation ($a_{\text{solute}} = 1$) σ (S-cm)	σ_0 (S-cm^{-1})	ϕ_c
Water	60	$40 \pm 10 \times 10^{-3}$	0.57 ± 0.15	0.1
Water	80	$70 \pm 15 \times 10^{-3}$	0.77 ± 0.20	0.1
Methanol	40	$9.8 \pm 3 \times 10^{-3}$	0.059 ± 0.012	0.1
Methanol	60	$15 \pm 4 \times 10^{-3}$	0.084 ± 0.020	0.1
Ethanol	40	$2.4 \pm 1.0 \times 10^{-3}$	0.012 ± 0.004	0.1
Ethanol	60	$5 \pm 1.5 \times 10^{-3}$	0.024 ± 0.004	0.1

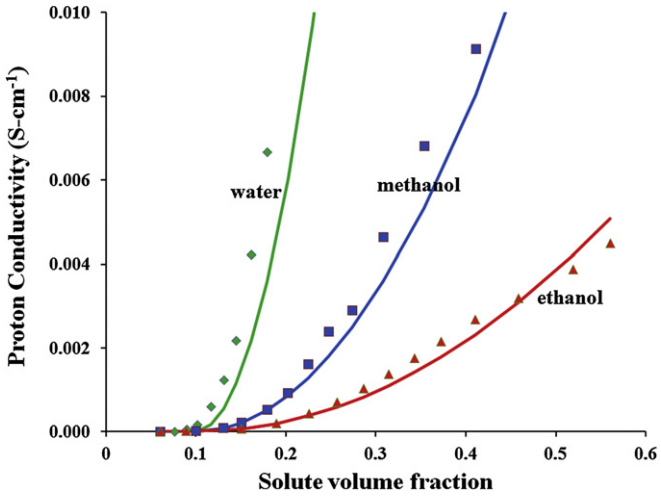

Fig. 5. Proton conductivity of EW1100 H+-Nafion at 60 °C as a function of hydrophilic volume fraction for methanol (squares), ethanol (triangle) and water (diamonds) sorption. The solid lines through the data are the best fit to the percolation model $\sigma(\lambda_{solute}) = \sigma_0(\phi_+ - \phi_c)^2$ with model parameters listed in Table 1.

desorption. The time for the same fractional mass gain from methanol sorption was approximately twice the time for an equivalent mass loss by methanol desorption. The sorption rate per unit mass of Nafion decreased with increasing membrane thickness.

Mass uptake showed universal scaling for different membrane thickness when plotted as a function of time/(membrane thickness) indicative of interfacial mass transport being the limiting resistance [22]. The graphs for scaling of mass uptake are provided in the Supplementary material. The rate of methanol sorption increased with temperature over the range of 30–60 °C (graph included in supplemental materials). The rate of methanol sorption doubled between 30 °C and 60 °C. These results for methanol sorption/desorption are qualitatively identical to the results previously reported for water sorption/desorption.

3.3. Methanol and ethanol pervaporation through Nafion

The pervaporation flux (permeation from liquid feed to vapor permeate) of methanol and ethanol through Nafion membranes with different thickness was measured at different nitrogen sweep

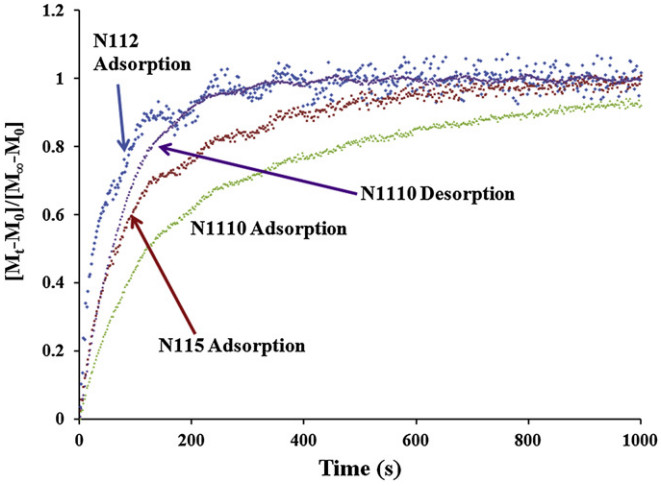

Fig. 6. Methanol sorption/desorption at 60 °C from 1100 EW H+-Nafion with different film thicknesses.

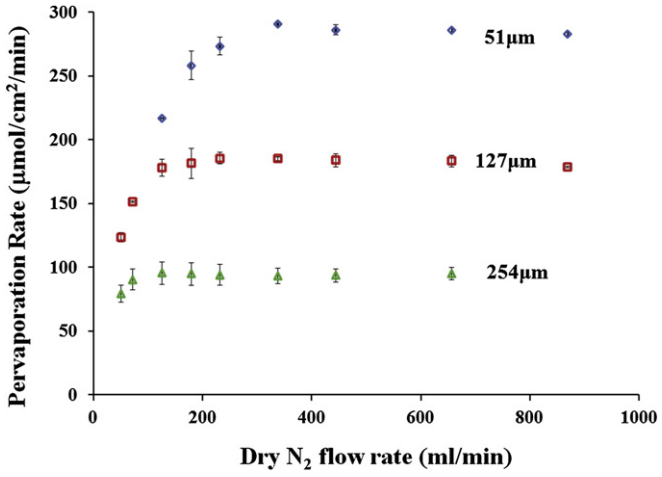

Fig. 7. Methanol pervaporation flux through Nafion 112, 115 and 1110 membranes at 22 °C as a function of nitrogen flow rate at the permeate side.

flow rates at the permeate side of the membrane. The methanol flux through N112 (51 μm dry thickness), N115 (127 μm dry thickness) and N1110 (254 μm dry thickness) as functions of the nitrogen sweep rate at 22 °C is shown in Fig. 7. The flux increases with gas flow rate and reaches a limiting flux at nitrogen sweep rates >200 mL/min. The limiting flux decreases with increasing membrane thickness. The limiting pervaporation flux measured for methanol and ethanol as functions of membrane thickness and temperature is summarized in Table 2. Pervaporation flux increased with increasing temperature and decreased with increasing membrane thickness. At the same temperature the pervaporation flux of methanol is greater than ethanol.

3.4. Methanol vapor permeation

Methanol permeation through Nafion was measured for three different vapor activities at the feed side. The limiting flux was determined by increasing the nitrogen gas flow at the permeate side. Table 3 summarizes the limiting permeation fluxes for the different solute vapor feed activities.

The maximum permeation fluxes for water and methanol across a Nafion 115 membrane at 22 °C and 60 °C are plotted as functions of feed side water activity in Fig. 8. Because the diffusion coefficient is a function of solute activity and the solute activity varies across the membrane there is no simple analytical model that correlates feed side solute activity to the permeation flux. The data were fit to simple exponential functions solute flux = $s\exp[b \times a_{solute}]$, where s is a function of temperature, membrane thickness and solute and b is only a function of solute. Methanol has a lower limiting permeation flux than water through Nafion at the same solute activity. Methanol and water permeation fluxes both increase with

Table 2
Maximum pervaporation fluxes of methanol and ethanol through Nafion membranes.

Solute	Temperature	Pervaporation flux μmole-cm^{-2}-min^{-1}		
		Membrane thickness		
		112 (51 μm)	115 (127 μm)	1110 (254 μm)
Methanol	22	276 ± 23	183 ± 12	114 ± 13
Methanol	40	412 ± 33	255 ± 27	161 ± 11
Methanol	60	642 ± 44	413 ± 41	232 ± 23
Ethanol	22	98 ± 8	43 ± 5	23 ± 3

Table 3
Methanol vapor permeation through Nafion.

$a^{feed}_{methanol}$	T (°C)	Methanol flux (μmol-cm^{-2}-min^{-1})		
		Membrane thickness		
		112 (51 μm)	115 (127 μm)	1110 (254 μm)
0.3	22	9.9 ± 0.9	5.5 ± 0.7	2.7 ± 0.4
0.5	22	29 ± 3	18 ± 1	8.7 ± 1.4
0.8	22	75 ± 11	55 ± 6	29 ± 1
0.3	40	19 ± 3	9.9 ± 1.0	4.9 ± 0.4
0.5	40	45 ± 3	27 ± 4	14 ± 0.4
0.8	40	158 ± 18	90 ± 1	56 ± 3
0.3	60	37 ± 3	20 ± 3	9.6 ± 1.3
0.5	60	89 ± 7	49 ± 3	25 ± 3
0.8	60	264 ± 25	139 ± 5	81 ± 14

temperature and increase exponentially with feed side solute activity.

4. Discussion

Sorption, proton conductivity, swelling and transport of water in H+Nafion have been extensively studied [21,30–36]. We report here similar measurements for methanol and ethanol to identify similarities and differences between alcohols and water interacting with H+Nafion. The sorption and transport characteristics of Nafion with methanol and ethanol sorption are remarkably similar to those of Nafion with water sorption. The sorption isotherms, sorption swelling, and proton conductivities as functions of solute activity follow nearly identical trends. The kinetics of sorption/desorption show the same qualitative trends for methanol as water. The dependence of pervaporation rate on membrane thickness is the one property where there was a distinct qualitative difference between alcohols and water. We suggest that the strong similarities of alcohol and water sorption and transport in H+-Nafion reflect the similarities of polar bonding interactions between OH groups of alcohols or water with the polar sulfonic acid groups of Nafion. Methanol, ethanol and water are all expected to produce similar microphase separated hydrophilic domains through which protons, water and alcohols are transported. The quantitative differences in sorption and transport of alcohols compared to water are suggested to reflect the differences in molecular size.

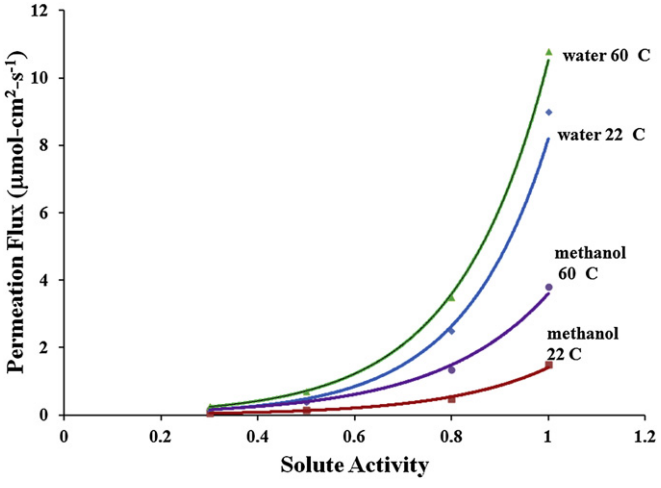

Fig. 8. Permeation flux of water and methanol through Nafion 115 at 22 and 60 °C. The lines through the data are given by solute flux = $s$exp[$b \times a_{solute}$]; $b_{methanol} = 4.4$ and $b_{water} = 5.6$ and $s_{methanol}$ (22 °C) = 0.012 μmol-cm^{-2} s^{-1}, $s_{methanol}$ (60 °C) = 0.043 μmol-cm^{-2} s^{-1}, s_{water} (22 °C) = 0.028 μmol-cm^{-2} s^{-1}, s_{water} (60 °C) = 0.048 μmol-cm^{-2} s^{-1}.

4.1. Sorption isotherms

Figs. 1 and 2 show that the sorption isotherms of methanol and ethanol have a similar functional dependence on solute activity as the water sorption isotherm. The sorption isotherms collapse to functions of solute activity, where the temperature dependence for sorption is captured by the standard state chemical potential of the solute. Wu et al. fit the water sorption isotherm to the solvation shell model given by Eq. (6), where K_0 is the equilibrium sorption constant for the first solvation shell, and K_1 is the equilibrium sorption constant for the second shell and beyond [37]. The best fits for water, methanol and ethanol sorption data to Eq. (6) were with four water molecules in the first solvation shell, consistent with the results obtained from excess volume of mixing described above. The sorption data for methanol and ethanol were fit to the solvation shell isotherm and the least square fit for the model parameters are given in Table 4. The equilibrium constants for the first solvation shell were similar for methanol, ethanol and water, and were 3–4 times larger than the equilibrium constant for the second solvation shell.

$$\lambda = \frac{\sum_{i=1}^{n_1} i(K_0 a_w)^i + (K_0 a_w)^{n_1}\left[\dfrac{n_1}{1-K_1 a_w} + \dfrac{1}{(1-K_1 a_w)^2}\right]}{\sum_{i=1}^{n_1}(K_0 a_w)^i + (K_0 a_w)^{n_1}\left[\dfrac{1}{1-K_1 a_w}\right]} \tag{6}$$

$$\begin{aligned} K_i &= K_0, \quad 1 \le i \le n_1 \\ K_i &= K_1, \quad n_1 < i \end{aligned} \tag{7}$$

The sorption isotherms and sorption swelling show two differences between the alcohols and water. (1) The maximum number of moles of solute sorbed decreased with increasing solute molar volume. This decrease in solute uptake is reflected in smaller values of K_1; $K_{1,ethanol} < K_{1,methanol} < K_{1,water}$. (2) The swelling volume increases with solute molar volume. The effect of solute molar volume on sorption and swelling is intuitively expected. Sorption of polar solutes into Nafion involves the exothermic solvation of the sulfonic acid by the polar solute and the endothermic expansion of the hydrophobic matrix surrounding the hydrophilic sulfonic acid domains. The larger molar volume of the alcohols ($\bar{V}_{water} = 18$ cm^3/mol $< \bar{V}_{methanol} = 40.4$ cm^3/mol $< \bar{V}_{ethanol} = 58.3$ cm^3/mol) will encounter greater resistance to swelling for the same number of sorbed molecules. It is surprising that the solvation energy of the alcohols is sufficient to produce greater swelling than water. Water is expected to be a better solvent for the ionic sulfonic acid groups of Nafion. We suggest that the substantial solvation by methanol and ethanol may in part be due to reduced interfacial energy between the hydrophobic matrix and hydrophilic domains. The interfacial energy between water and tetrafluoroethylene (TFE) is much more repulsive than the alcohol/TFE. The sessile drop contact angles of water and methanol with Teflon and Nafion reported by Goswami et al. are $\theta_{water/teflon} = 110°$; $\theta_{water/nafion} = 105°$;

Table 4
Solvation shell isotherm parameters for water, methanol and ethanol sorption isotherms in 1100 EW H+-Nafion.

Solute	n	K_0	K_1
Water (60 °C)	4	4.0	0.97
Water (80 °C)	4	3.7	0.96
Methanol (40 °C)	4	3.8	0.95
Methanol (60 °C)	4	3.5	0.95
Ethanol (40 °C)	4	3.2	0.92
Ethanol (60 °C)	4	2.8	0.92

$\theta_{methanol/teflon} = 20°$; $\theta_{methanol/nafion} = 20°$ [38]. The surface tension of water on Teflon is 4.8×10^{-5} kJ m^2, while the surface tension of methanol on Teflon is 1.5×10^{-5} kJ m^2. Swelling the hydrophilic domains with alcohols will require less energy than swelling with water. Additional factors such as hydrogen bonding and the dipole-dipole interactions will also alter the energy of solvation, but those interactions would be expected to result in less sorption of alcohols compared to water.

The sorption isotherms for water, methanol and ethanol vapor all show universal scaling of mass and volume uptake with solute activity; the temperature dependence is very small after scaling the solute partial pressure with the vapor pressure. These results indicate that water, methanol and ethanol sorption into the hydrophilic domains is similar to vapor/liquid condensation. The free energy of water and alcohol vapor sorption into Nafion is not much different than the free energy of vapor/liquid condensation.

4.2. Proton conductivity

Recently Wu et al. showed that the percolation threshold for proton conductivity in ionomers could be identified from a plot of conductivity vs. hydrophilic volume fraction, where the hydrophilic domain was assumed to consist of the sulfonic acid groups and sorbed water [37]. Fig. 5 shows the application of a similar analysis to identify the proton conductivity percolation threshold with alcohol sorption, assuming the hydrophilic volume fraction consists of the sulfonic acid groups and the alcohol molecules. The results show that the percolation threshold for proton conductivity was the same within experimental error for methanol, ethanol and water. The hydrophilic volume fraction percolation threshold was $\phi_+ \sim 0.1$. This low value for the percolation threshold indicates that the hydrophilic domains should be oblates (either rods or plates); if the hydrophilic domains were spherical the percolation threshold would be 0.3 [39]. The similarity of the percolation threshold for water and alcohols suggests that the shape of the hydrophilic domains at low solute activity (and hence low solute content) is determined by the sulfonic acid domain structure in solute free Nafion.

In fitting the conductivity data to percolation theory the exponent was fixed and the percolation threshold was found by least squares fit to the data above the threshold. Because Nafion has a distribution of domain shapes the percolation analysis is semi-quantitative; we chose not to overanalyze the data by attempting to extract values of both the exponent and percolation threshold. The conductivity data indicates that there must be oblate hydrophilic domains, but the conductivity data cannot by itself determine the distribution of domain shapes and sizes.

The proton conductivities of Nafion equilibrated with saturated vapors or water, methanol and ethanol at 60 °C were 0.06, 0.02 and 0.005 S cm^{-1} respectively. Above the percolation threshold for proton conduction (which occurs at solute activity of ~0.2) the proton conductivity followed the same trend. Proton conductivity for the three solutes at the same volume fraction follow the trend that $\sigma_{H+,water} > \sigma_{H+,methanol} > \sigma_{H+,ethanol}$. There are two obvious contributions to the decrease in proton conductivity with the alcohols. Firstly, alcohols are less polar than water which is expected to result in reduced ionization of the sulfonic acid. Secondly, water can form a hydrogen bonded network through which protons may be transported by hopping. Hopping is less important with alcohols which could also reduce proton conductivity.

At low solute activity the proton conductivity was greater for Nafion with sorbed alcohols than Nafion with sorbed water; at solute activity of 0.02 the proton conductivities of Nafion with sorbed water, methanol and ethanol were 1.5×10^{-5}, 1×10^{-4} and 7×10^{-5} S cm^{-1} respectively. At low solute content the number of water or alcohol molecules is the same in the first solvation shell. The larger molar volume of the alcohols results in larger hydrophilic domains which may facilitate proton transport. Unfortunately the experimental transport data is not able to separate the different contributions to proton transport.

4.3. Sorption/desorption kinetics

The rate of methanol sorption from saturated vapor was slower than the rate of methanol desorption. The rates of methanol sorption and desorption both increased with increasing temperature. And the normalized mass change scaled with (time)/(membrane thickness) indicative of an interfacial mass transport process being rate limiting for water sorption. All three of these characteristic features of solute sorption/desorption were reported by Satterfield and Benziger for water sorption into H+Nafion membranes [22]. The qualitative similarity suggests that the kinetics of methanol sorption from saturated vapor is limited by the same physical processes as found for water sorption listed below.

1. Initial solute uptake is limited by solute diffusion in the membrane. At low solute content diffusion is slow.
2. The second stage of solute uptake is limited by membrane swelling to accommodate the increased volume of the hydrophilic domains. At moderate solute concentrations solute diffusion is faster than the kinetics to swell the membrane to accommodate more solute. Swelling proceeds from the membrane surface inward. The kinetics for the moving swelling front is similar to mass transport across a moving interface.
3. Desorption of solute is limited by diffusion to the membrane/vapor interface followed by interfacial transport into the vapor. The kinetics of shrinking the hydrophilic domains does not affect desorption of solute. The difference between sorption and desorption are analogous to blowing up and deflating a balloon.

4.4. Pervaporation of methanol and ethanol through Nafion

Methanol and ethanol pervaporation through Nafion decreased with membrane thickness. Increasing the membrane thickness by a factor of 5 decreased the pervaporation flux by a factor of 3. This is in contrast to the pervaporation flux of water through 1100 EW H+Nafion membranes; the pervaporation water flux decreased by less than a factor of 1.5 when the membrane thickness increased from 50 to 250 μm. Interfacial transport of water across the membrane/vapor interface at the permeate side has been suggested to cause water pervaporation to be primarily limited by interfacial transport. In contrast methanol and ethanol pervaporation fluxes through Nafion appear to be primarily limited by diffusion through the membrane.

4.5. Permeation of methanol vapor through Nafion

Methanol and water vapor permeation fluxes through Nafion membranes both decreased with increasing membrane thickness. The primary resistance to vapor permeation of both water and methanol appears to be diffusion in the membrane.

Steady state pervaporation and permeation across membranes involves three transport steps in series shown in Eq. (8): (i) interfacial transport from the feed (either vapor or liquid) into the membrane; (ii) diffusion across the membrane; and (iii) interfacial transport from the membrane into the vapor permeate stream. Overall transport can be approximated by a linear model where the flux of each step must be the same as shown in Eq. (8), where k_f and

k_p are interfacial transport coefficients into and out of the membrane, D is the diffusivity of solute in the membrane, c_0 is the concentration of solute in the membrane at saturation solute activity and $t_{membrane}$ is the membrane thickness.

$$\text{flux} = k_f\left(a^{feed}_{solute} - a^{feed}_{membrane}\right) = \frac{c_0 D}{t_{membrane}}\left(a^{feed}_{membrane} - a^{permeate}_{membrane}\right) = k_p\left(a^{permeate}_{membrane} - a^{permeate}_{solute}\right) \quad (8)$$

The solute activities in the membrane are not directly measured; only the feed and permeate solute activities are directly measured. Eq. (8) can be arranged to express the flux in terms of the transport parameters and the feed and permeate solute activities.

$$\text{flux} = \frac{\frac{c_0 D}{t_{membrane}} k_f k_p}{\frac{c_0 D}{t_{membrane}}\left(k_f + k_p\right) + k_f k_p}\left(a^{feed}_{solute} - a^{permeate}_{solute}\right) \quad (9)$$

The limiting solute flux occurs with infinite permeate gas flow when the solute activity in the permeate stream approaches zero. Eq. (9) can be rearranged at the limiting flux; Eq. (10) relates the ratio of the feed activity to the limiting flux to the diffusion coefficient and interfacial transport coefficients.

$$\frac{a^{feed}_{solute}}{(\text{flux})_{limiting}} = \frac{t_{membrane}}{c_0 D} + \frac{1}{k_f} + \frac{1}{k_p} \quad (10)$$

Assuming that the diffusivity and interfacial transport coefficients are not functions of composition, the product c_0D and the sum $(1/k_f + 1/k_p)$ can be determined from a series of measurements of the limiting flux with different membrane thickness at fixed feed activity and temperature. Fig. 9 is a plot of feed activity divided the limiting flux as a function of membrane thickness for water, methanol and ethanol pervaporation at different temperatures. Fig. 10 is a similar plot for vapor permeation experiments. The data at fixed temperature and feed solute activity regress to straight lines. The slopes of these lines are inversely related to the solute diffusivity in the membrane ($c_0D = 1/\text{slope}$) and the intercept of the lines are inversely related to the interfacial transport coefficients.

The pervaporation data for methanol, ethanol and water (data previously reported by Majsztrik et al.[40]) is plotted in Fig. 9 as suggested by Eq. (10). The slopes and intercepts were regressed to determine $\text{slope} = 1/(c_0D)$ and $\text{intercept} = 1/k_p + 1/k_f$ at the different temperatures. The interfacial transport resistance at the liquid membrane interface was assumed to be negligible for pervaporation, e.g. $k_f \to \infty$, hence for pervaporation experiments the intercepts in Fig. 9 are equal to the reciprocal of the interfacial transport coefficient at the permeate side, $1/k_p$. The membrane solute concentration at saturation, c_0, was determined from the sorption isotherms as $a_{solute} \to 1$. See Figs. 1 and 2 and Eq. (11): $c_{0,water} = 2.5 \times 10^{-2}$ mol/cm^3; $c_{0,methanol} = 1.3 \times 10^{-2}$ mol/cm^3; $c_{0,ethanol} = 0.95 \times 10^{-2}$ mol/cm^3.

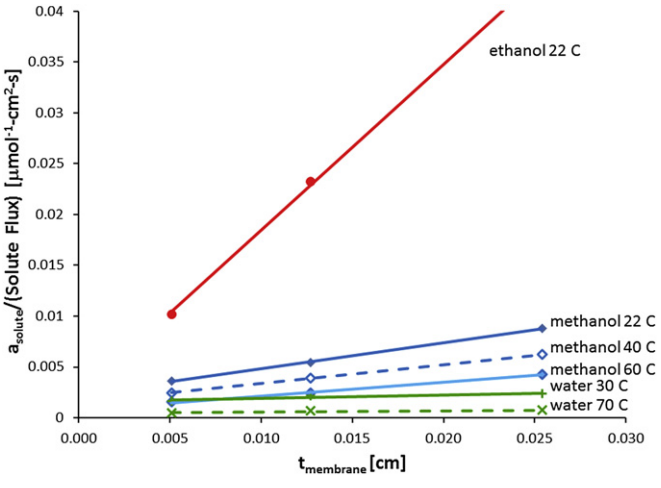

Fig. 9. Plot of Eq. (10) for pervaporation experiments with Nafion 112, Nafion 115 and Nafion 1110 membranes. Data sets are constant temperature are fit to straight lines.

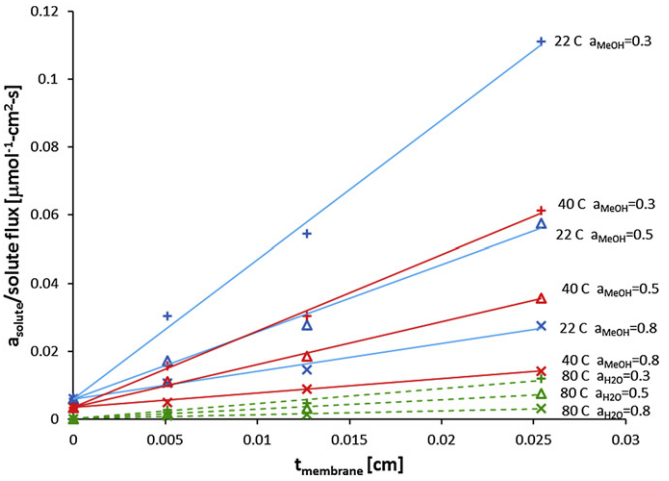

Fig. 10. Plot of Eq. (10) for vapor permeation experiments of water and methanol through Nafion 112, 115 and 1110. Data sets at constant temperature and constant solute activity are fit to straight lines.

$$c_0 = \frac{\lambda \rho_{Nafion}}{EW\left[(1 + \varepsilon(a_{solute} = 1))^3 - 1 + \phi_0\right]} \quad (11)$$

Diffusion coefficients and interfacial transport coefficients from the pervaporation experiments are summarized in Table 5. The self-diffusion coefficient for water in 1100 EW H+Nafion determined by Zhao et al. [24] is included in parentheses in Table 5. The diffusion coefficients for water agree with the self-diffusion coefficients within a factor of 2. This is good agreement, particularly considering the assumption made here of uniform diffusivity in the membrane.

The diffusion coefficients follow the trend that diffusivity decreases with increasing molar volume: $D_{water} > D_{methanol} > D_{ethanol}$. The results for methanol and water both show that diffusivity increases with increasing temperature. The interfacial mass transport coefficients (k_p) increase with increasing temperature for both methanol and water. The interfacial transport coefficients for methanol and water had similar values at the same

Table 5
Diffusivity and interfacial transport coefficients from pervaporation fluxes.

Solute	Temperature (°C)	D_{solute} (cm^2-s^{-1}) $\times 10^6$	k_p (μmol-cm^{-2}-min^{-1})[b]
Methanol	22	5.2 ± 1.0	440
Methanol	40	7.2 ± 1.3	670
Methanol	60	9.7 ± 1.6	1300
Ethanol	22	1.1 ± 0.3	380
Water	30	12 ± 6 (4.3)[a]	700
Water	50	16 ± 8 (8.5)[a]	1400
Water	70	24 ± 12 (15.5)[a]	1700

[a] Values in parentheses are self-diffusion coefficients from Zhao et al. [24].
[b] The errors on the k_p values are estimated to be a factor of 2.

temperature. The ratio of the interfacial transport resistance to the diffusional resistance, $c_0D/t_{membrane}k_p$, is larger for water than methanol, consistent with the experimental observation that the pervaporation flux of methanol through Nafion had a much larger dependence on membrane thickness than did the pervaporation water flux.

The vapor permeation experiments were analyzed in the same fashion as the pervaporation experiments, except the interfacial transport resistance at the feed side could not be neglected with a membrane/vapor interface. We assumed that membrane/vapor interfacial transport coefficients were the same at both the feed and permeate, $k_f \approx k_p$. With that assumption the intercept from the plot of $a^{feed}_{solute}/(\text{flux})$ vs. $t_{membrane}$ is equal to $2/k_p$. Fig. 10 plots the permeation data for methanol and water as suggested by Eq. (10). The data in Fig. 10 were grouped by temperature and feed side solute activity. The data at constant feed side activity and temperature were regressed to straight lines where the $1/\text{slope} = c_0D$, and $1/\text{intercept} = 2/k_p$. c_0D and k_p were evaluated at the different temperatures and feed solute activity; the results for the diffusivity and interfacial transport coefficients from vapor permeation experiments are summarized in Table 6.

Fig. 10 shows that at a given temperature the lines at different feed side solute activities extrapolate back to the same intercept. Diffusivity changes with solute activity, but the vapor/membrane interfacial transport coefficients appear to be functions only of temperature and not solute activity. The diffusivities of water and methanol both decrease with decreasing water activity and decreasing temperature.

The vapor/membrane interfacial transport coefficients increase with increasing temperature. But the vapor/membrane interfacial transport coefficients show a negligible dependence on solute activity. The data is sparse but the interfacial transport coefficients for water and methanol appear to scale with vapor pressure. The scaling of the interfacial transport coefficients with vapor pressure is consistent with the vaporization-exchange model for interfacial transport proposed by Monroe et al. [41].

4.6. Correlation of proton transport and solute diffusion

Methanol, ethanol and water transport through Nafion are remarkably similar. Alcohols and water both swell hydrophilic domains and diffuse through the hydrophilic domains. Water and alcohols also ionize the sulfonic acid groups in Nafion and facilitate proton transport. Both proton transport and solute diffusion have been assumed to occur in the hydrophilic channels of Nafion. A percolation threshold for proton conductivity was identified for water, methanol and ethanol sorption. One might expect a similar percolation threshold for solute diffusion.

Table 6
Diffusivity and interfacial transport coefficients from permeation fluxes.

Solute	Temperature (°C)	Solute activity	D_{solute} (cm^2-s^{-1}) × 10^6	k_p (μmol-cm^{-2}-min^{-1})[b]
Methanol	22	0.3	0.33 ± 0.2	270
Methanol	22	0.5	0.67 ± 0.3	390
Methanol	22	0.8	1.6 ± 0.7	380
Methanol	40	0.3	0.59 ± 0.3	610
Methanol	40	0.5	1.1 ± 0.5	490
Methanol	40	0.8	3.0 ± 1.2	690
Methanol	60	0.3	1.2 ± 0.6	1300
Methanol	60	0.5	1.9 ± 0.9	1300
Methanol	60	0.8	4.0 ± 1.4	1400
Water	30	0.3	0.74 ± 0.4 (0.38)[a]	570
Water	30	0.5	1.0 ± 0.5 (1.1)[a]	440
Water	30	0.8	1.6 ± 0.8 (2.8)[a]	570
Water	80	0.3	1.6 ± 0.8 (1.8)[a]	1900
Water	80	0.5	2.3 ± 1.1 (5.0)[a]	1900
Water	80	0.8	6.4 ± 3.0 (12.8)[a]	1900

[a] Values in parentheses are self-diffusion coefficients from Zhao et al. [24].
[b] The errors on the k_p values are estimated to be a factor of 2.

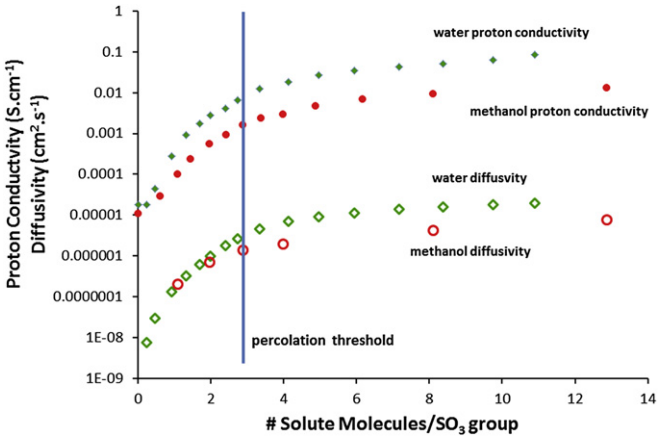

Fig. 11. Proton conductivity and methanol and water diffusivity in 1100 EW H+Nafion as functions of solute sorption. The percolation threshold for hydrophilic volume fraction of water of 0.1 is highlighted with the vertical line.

Fig. 11 is a logarithmic plot of the proton conductivities in H+Nafion as a function of water and methanol sorption. The percolation threshold for proton conduction identified in Fig. 5 occurs at $\lambda \approx 3$–4 solute molecules per SO_3 group. The diffusion coefficients for water and methanol in Nafion have been added to this figure. The diffusion coefficients for water are the data presented here combined with the more extensive data obtained by Zhao et al. [24] The diffusion coefficients for methanol are those obtained in the experiments reported here (there are many fewer points). The diffusion coefficients for methanol and water parallel the proton conductivity for sorption of methanol and water respectively. Although this is not definitive proof, this correlation does support to the assumption that proton conduction and solute diffusion occur by related processes in the hydrophilic channels of Nafion.

5. Conclusions

The sorption and transport of methanol and ethanol into 1100 EW H+-Nafion has been compared to water sorption and transport. Alcohols and water both interact primarily with the sulfonic acid groups forming percolated networks through which protons, alcohols and water are transported. The sorption and transport properties for methanol, ethanol and water are qualitatively similar. The quantitative differences are primarily due to differences in molar volumes. The key results may be summarized as follows:

1. Methanol, ethanol and water sorb in Nafion by forming solvation shells around the sulfonic acid group. The first solvation shell is four strongly bound polar molecules; the second solvation shell and beyond are less strongly bound.
2. Fewer methanol and ethanol molecules are sorbed by Nafion than water molecules because of greater energy required to swell the hydrophilic domains to accommodate the larger alcohol molecules.
3. The percolation threshold for proton conductivity in Nafion occurs at a hydrophilic volume fraction threshold of 0.1 for methanol, ethanol and water. Proton conductivity decreases with increasing solute molar volume ($\sigma_{H+,water} > \sigma_{H+,methanol} > \sigma_{H+,ethanol}$).

4. Methanol sorption into Nafion is slower than methanol desorption. Methanol sorption and desorption increase with increasing temperature from 22 °C to 60 °C.
5. Diffusion of alcohols through Nafion membranes is the primary resistance to pervaporation and vapor permeation.
6. The diffusivity of methanol in Nafion is less than the diffusivity of water. The diffusivity of methanol in Nafion increases with increasing methanol activity and increasing temperature.

Acknowledgment

This work was supported by the National Science Foundation MRSEC Program through the Princeton Center for Complex Materials (GS1) (DMR-0819860). Nicole Caro was supported as a Research Experience for Teachers program through the NSF MRSEC program.

Appendix. Supplementary data

Supplementary data related to this article can be found online at doi:10.1016/j.polymer.2012.01.050

References

[1] Larminie J, Dicks A. In: Fuel cell systems explained. 2nd ed. New York: Wiley; 2003.
[2] Deluca NW, Elabd YA. Journal of Polymer Science Part B – Polymer Physics 2006;44(16):2201–25.
[3] Neburchilov V, Martin J, Wang HJ, Zhang JJ. Journal of Power Sources 2007; 169(2):221–38.
[4] Tsai CE, Hwang BJ. Fuel Cells 2007;7(5):408–16.
[5] Rivin D, Meermeier G, Schneider NS, Vishnyakov A, Neimark AV. Journal of Physical Chemistry B 2004;108(26):8900–9.
[6] Every HA, Hickner MA, McGrath JE, Zawodzinski TA. Journal of Membrane Science 2005;250(1-2):183–8.
[7] Hallinan DT, Elabd YA. Journal of Physical Chemistry B 2007;111(46):13221–30.
[8] Saito M, Tsuzuki S, Hayamizu K, Okada T. Journal of Physical Chemistry B 2006;110(48):24410–7.
[9] Gates CM, Newman J. AIChE Journal 2000;46(10):2076–85.
[10] Hietala S, Maunu SL, Sundholm F. Journal of Polymer Science Part B – Polymer Physics 2000;38(24):3277–84.
[11] Dimitrova P, Friedrich KA, Stimming U, Vogt B. Solid State Ionics 2002;150(1, 2): 115–22.
[12] Pivovar BS, Wang YX, Cussler EL. Journal of Membrane Science 1999;154(2): 155–62.
[13] Han JH, Liu HT. Journal of Power Sources 2007;164(1):166–73.
[14] Hikita S, Yamane K, Nakajima Y. Jsae Review 2001;22(2):151–6.
[15] Thomas SC, Ren X, Gottesfeld S, Zelenay P. Electrochimica Acta 2002;47(22, 23): 3741–8.
[16] Ren X, Springer TE, Gottesfeld S. Journal of the Electrochemical Society 2000; 147(1):92–8.
[17] Ren XM, Springer TE, Zawodzinski TA, Gottesfeld S. Journal of The Electrochemical Society 2000;147(2):466–74.
[18] Kim YM, Park KW, Choi JH, Park IS, Sung YE. Electrochemistry Communications 2003;5(7):571–4.
[19] Zhou XY, Weston J, Chalkova E, Hofmann MA, Ambler CM, Allcock HR, et al. Electrochimica Acta 2003;48(14–16):2173–80.
[20] Majsztrik P, Bocarsly A, Benziger J. Journal of Physical Chemistry B 2008; 112(51):16280–9.
[21] Satterfield MB, Benziger JB. Journal of Physical Chemistry B 2008;112(12): 3693.
[22] Satterfield MB, Benziger JB. Journal of Polymer Science Part B – Polymer Physics 2009;47(1):11–24.
[23] Majsztrik PW, Bocarsly AB, Benziger JB. Macromolecules 2008;41(24):9849–62.
[24] Zhao QA, Majsztrik P, Benziger J. Journal of Physical Chemistry B 2011; 115(12):2717–27.
[25] Satterfield MB, Majsztrik PW, Ota H, Benziger JB, Bocarsly AB. Journal of Polymer Science B 2006;44:2327–45.
[26] Majsztrik PW, Bocarsly AB, Benziger JB. Review of Scientific Instruments 2007; 78(10).
[27] Vishnyakov A, Neimark AV. Journal of Physical Chemistry B 2000;104(18): 4471–8.
[28] Jalani NH, Cho PG, Datta R. Solid State Ionics 2004;175(1–4):815–7.
[29] Van Krevelen DW. In: Properties of polymers. 3rd ed. New York: Elsevier; 1990.
[30] Ge S, Li X, Yi B, Hsing I. Journal of Electrochemical Society 2005;152(6):A1149.
[31] Hallinan DT, Elabd YA. Journal of Physical Chemistry B 2009;113(13): 4257–66.
[32] Majsztrik P, Bocarsly A, Benziger J. Journal of Physical Chemistry B 2008; 112(51):16280–9.
[33] Majsztrik PW, Satterfield MB, Bocarsly AB, Benziger JB. Journal of Membrane Science 2007;301:93.
[34] Monroe CW, Romero T, Merida W, Eikerling M. Journal of Membrane Science 2008;324(1, 2):1–6.
[35] Rivin D, Kendrick CE, Gibson PW, Schneider NS. Polymer 2001;42(2):623–35.
[36] Zawodzinski TA, Derouin C, Radzinski S, Sherman RJ, Smith VT, Springer TE, et al. Journal of Electrochemical Society 1993;140:1041.
[37] Wu X, Wang X, He G, Benziger J. Journal of Polymer Science Part B: Polymer Physics 2011;49(20):1437–45.
[38] Goswami S, Klaus S, Benziger J. Langmuir 2008;24(16):8627–33.
[39] Torquato S. Random heterogeneous materials. Microstructure and macroscopic properties. New York: Springer; 2002.
[40] Majsztrik PW, Bocarsly AB, Benziger J. Journal of Physical Chemistry B 2008; 112(51):16,280–16,289.
[41] Monroe CW, Romero T, Merida W, Eikerling M. Journal of Membrane Science 2008;324(1, 2):1–6.